

# Effect of Pulse Duration on Size and Character of the Lesion in Retinal Photocoagulation

ATul Jain, MD; Mark S. Blumenkranz, MD; Yannis Paulus, BA; Michael W. Wiltberger, AAS; Dan E. Andersen, BS; Phil Huie, MS; Daniel Palanker, PhD

**Objective:** To systematically evaluate the effects of laser beam size, power, and pulse duration of 1 to 100 milliseconds on the characteristics of ophthalmoscopically visible retinal coagulation lesions.

**Methods:** A 532-nm Nd:YAG laser was used to irradiate 36 retinas in Dutch Belt rabbits with retinal beam sizes of 66, 132, and 330  $\mu\text{m}$ . Lesions were clinically graded 1 minute after placement, their size measured by digital imaging, and their depth assessed histologically at different time points.

**Results:** Retinal lesion size increased linearly with laser power and logarithmically with pulse duration. The width of the therapeutic window, defined by the ratio of the threshold power for producing a rupture to that of a mild coagulation, decreased with decreasing pulse durations. For 132- and 330- $\mu\text{m}$  retinal beam sizes, the therapeutic window declined from 3.9 to 3.0 and 5.4 to 3.7,

respectively, as pulse duration decreased from 100 to 20 ms. At pulse durations of 1 millisecond, the therapeutic window decreased to unity, at which point rupture and a mild lesion were equally likely to occur.

**Conclusions:** At shorter pulse durations, the width and axial extent of the retinal lesions are smaller and less dependent on variations in laser power than at longer durations. The width of the therapeutic window, a measure of relative safety, increases with the beam size.

**Clinical Relevance:** Pulse durations of approximately 20 milliseconds represent an optimal compromise between the favorable impact of speed, higher spatial localization, and reduced collateral damage on one hand, and sufficient width of the therapeutic window ( $> 3$ ) on the other.

*Arch Ophthalmol.* 2008;126(1):78-85

**T**HE TREATMENT PARAMETERS for retinal photocoagulation have remained relatively constant since the first description of an argon laser (514-nm wavelength) coupled to a slitlamp delivery system in 1970.<sup>1</sup> The 3 separate but interdependent variables available to the clinician are the beam size, power, and duration of the pulse. Typically, for diabetic retinopathy, retinal vascular applications, and the treatment of retinal breaks, the retinal laser spot sizes range from 100 to 500  $\mu\text{m}$ ; the pulse durations, from 100 to 200 milliseconds; and the power, from 100 to 750 mW. The clinical appearance of the retinal lesions in these applications ranges from mild gray to a moderate white.<sup>2</sup> For the thermal destruction of tumors and extrafoveal choroidal neovascular membranes, somewhat longer-duration lesions, ranging from 200 to 500 milliseconds, and longer wavelengths in the yellow-red spectrum are often used.<sup>3</sup>

One of the earliest experimental studies demonstrating the feasibility of retinal photocoagulation by a ruby laser re-

ported a nonlinear correlation between the incident energy and the diameter of the retinal lesion.<sup>4</sup> Modeling of retinal heating with pulsed lasers has predicted an increase in the width and depth of the coagulated zone with increasing pulse durations.<sup>5</sup> Exposures from 10 to 50 milliseconds have been shown to reduce pain associated with photocoagulation.<sup>5</sup> It has also been observed that the safety margin between retinal coagulation and hemorrhage (ie, the ratio of threshold powers of these effects) produced by argon lasers (488 and 514 nm) decreased with decreasing pulse duration from 500 to 10 milliseconds, and with decreasing laser spot size.<sup>6</sup> The safety margin for 500- $\mu\text{m}$  spot size at 10 milliseconds corresponded to approximately a factor of 2.<sup>6</sup> On the other hand, no such tendencies have been reported with a near-infrared diode laser (805 and 840 nm).<sup>6</sup> In another study, the safety margin between the retinal blanching and hemorrhage with an argon laser ( $\lambda = 514$  nm) was found to decrease even faster; it became approximately 1 at 11-millisecond exposures.<sup>7</sup> Most of the subsequent experimental studies of laser treat-

**Author Affiliations:** Department of Ophthalmology, Stanford University, Stanford, California (Drs Jain, Blumenkranz, and Palanker and Mr Huie); Stanford University School of Medicine (Mr Paulus); and OptiMedica Corp, Santa Clara, California (Messrs Wiltberger and Andersen).

ment parameters during the ensuing 2 decades principally focused on the influence of wavelength and power on the nature of the retinal lesion at pulse durations in the range of 100 to 200 milliseconds.<sup>8-10</sup>

More recently, localized retinal damage has been achieved with micropulse photocoagulation, where a train of microsecond pulses is applied to the same spot. It has been shown that retinal damage can be localized to retinal pigment epithelium (RPE) if a low duty-factor sequence of 5-microsecond pulses is applied, minimizing heat accumulation.<sup>11</sup> However, the application of a relatively high duty factor (5%-15%) can lead to significant heat accumulation and result in retinal damage with energy thresholds similar to that of a continuous-wave laser.<sup>12,13</sup> Recently, there has been increasing interest in the use of even shorter duration pulses (200 nanoseconds to 1.7 microseconds) for retinal therapeutic applications. With this approach, termed *selective retinal therapy*, laser effects are confined to the RPE, with relative sparing of the adjacent photoreceptors and choriocapillaris.<sup>14,15</sup> Treatment with such lasers does not produce an immediate ophthalmoscopically visible retinal lesion at energies corresponding to selective damage of the RPE.<sup>15</sup> It was also discovered that the mechanism of cellular injury to the RPE changes as pulse durations decrease below 50 microseconds.<sup>16</sup> At longer pulses, damage is observed to be primarily thermal, while, with pulse durations shorter than 50 microseconds, cellular injury is mainly attributed to mechanical rupture by the transient vapor bubbles formed around melanosomes.

A new method of retinal photocoagulation called *pattern scanning laser* (PASCAL; OptiMedica Corp, Santa Clara, California) has recently been introduced, in which patterns of 4 to 56 pulses are applied in less than 1 second, using a scanning laser with pulse durations of 10 to 30 milliseconds.<sup>17</sup> With this system, the final size of the retinal lesion is strongly affected by the pulse duration and power, to a greater extent than was commonly seen clinically or documented in the literature for conventional (100-millisecond range) systems. These observations led us to systematically study the influences of pulse duration in the range of 1 to 100 milliseconds and power in the range of 50 to 400 mW on the size and nature of the retinal lesion. We also questioned whether it was possible to experimentally determine a preferred range of pulse durations that optimized the speed of the treatment and spatial localization of the visible lesions while minimizing the potential for photomechanical injury or rupture.

## METHODS

### INSTRUMENT

A modified slitlamp (model 950; Costruzione Strumenti Oftalmici, Florence, Italy) was used to support the laser scanning device and provide a view of the fundus. The optical radiation from a diode-pumped continuous-wave frequency-doubled (532-nm wavelength) Nd:YAG laser (model 58-GOS-305; Melles Griot, Carlsbad, California) was coupled into a multimode step index optical fiber (core diameter, 50  $\mu\text{m}$ ; numerical aperture, 0.22; model M14L05; Thorlabs, Newton, New Jer-

sey). The exit surface of the fiber was telecentrically imaged through the scanning system onto the retina with variable magnification, thus providing a variety of spot sizes with nominally top-hat intensity profiles. At the aerial image plane of the slitlamp microscope, the laser spot sizes measured 100, 200, and 500  $\mu\text{m}$ , with the laser intensity transition from 10% to 90% occurring over 3, 4, and 6  $\mu\text{m}$ , respectively. Variation of the beam intensity within the top-hat area did not exceed  $\pm 7\%$ . The frequency-doubled pulsed Nd:YAG laser has been shown to produce retinal coagulation equivalent to that of an argon green laser (514 nm) when a burst of high-repetition-rate pulses is applied, making the average effect equivalent to that of a continuous-wave laser.<sup>18-20</sup> Because of lower xanthophyll absorption at 532 nm, the inner retinal damage in the macular area is expected to be reduced compared with the damage produced by an argon laser.<sup>19</sup>

A 2.8-GHz dual core Pentium IV PC (model GX520; Dell Inc, Austin, Texas) computer running under Windows XP was used to support and monitor a field programmable gate array device (model PCI-7833R; National Instruments, Austin) that independently controlled and monitored the entire system with the use of dedicated reconfigurable hardware. A touch screen (model E153; Dell Inc, Austin) graphical user interface was used to control clinical system variables including spot size, laser power, pulse duration, and pattern geometry. Once clinical variables were appropriately selected, a foot pedal similar to those in standard photocoagulators was used to activate the laser.

## EXPERIMENTAL METHODS

Eighteen Dutch Belt rabbits (weight, 2-3 kg) were used in accordance with the Association for Research in Vision and Ophthalmology Statement Regarding the Use of Animals in Ophthalmic and Vision Research after approval from the Stanford University Animal Institutional Review Board. The rabbits were anesthetized with ketamine hydrochloride (35 mg/kg), xylazine (5 mg/kg), and glycopyrrolate (0.1 mg/kg), which were administered intramuscularly 15 minutes before the procedure. Pupillary dilation was achieved by 1 drop each of 1% tropicamide and 2.5% phenylephrine hydrochloride. Only 1 eye of each rabbit was treated at a time, unless the rabbit was to be immediately killed. We compared the effects of various laser powers, pulse durations, and beam sizes on the histologic character, size, and depth of the resultant retinal lesion. In measurements of the lesion sizes, at least 3 separate exposures were averaged. In measurements of the coagulation thresholds for retinal lesions of various grades, 8 to 16 separate lesions were administered and averaged for each graphical data point.

A standard retinal laser contact lens (Mainster, model OMRA-S; Ocular Instruments, Bellevue, Washington) was used to focus the laser on the rabbit fundus. Taking into account the combined magnifications of the contact lens and rabbit eye of 0.66,<sup>21</sup> the aerial images of 100, 200, and 500  $\mu\text{m}$  corresponded to retinal spot sizes of 66, 132, and 330  $\mu\text{m}$ , respectively. Rabbits were killed 1 hour, 1 day, or 1 week after treatment. Eyes were enucleated and fixed in 1.25% glutaraldehyde/1% paraformaldehyde in cacodylate buffer at pH 7.4. The eyes were then postfixated in osmium tetroxide, dehydrated with a graded series of ethanol, and embedded in an epoxy resin. Sections of 1  $\mu\text{m}$  in thickness were stained with toluidine blue and examined by light microscopy. Toluidine blue was used because of its efficacy in demonstrating retinal structural components and cellular architecture.<sup>22</sup>

The clinical appearance of the laser lesions was graded by a single observer (A.J.) within 20 seconds of delivering the laser pulse by means of the following scale: barely visible, mild, moderate, intense, very intense, and rupture. A barely visible le-

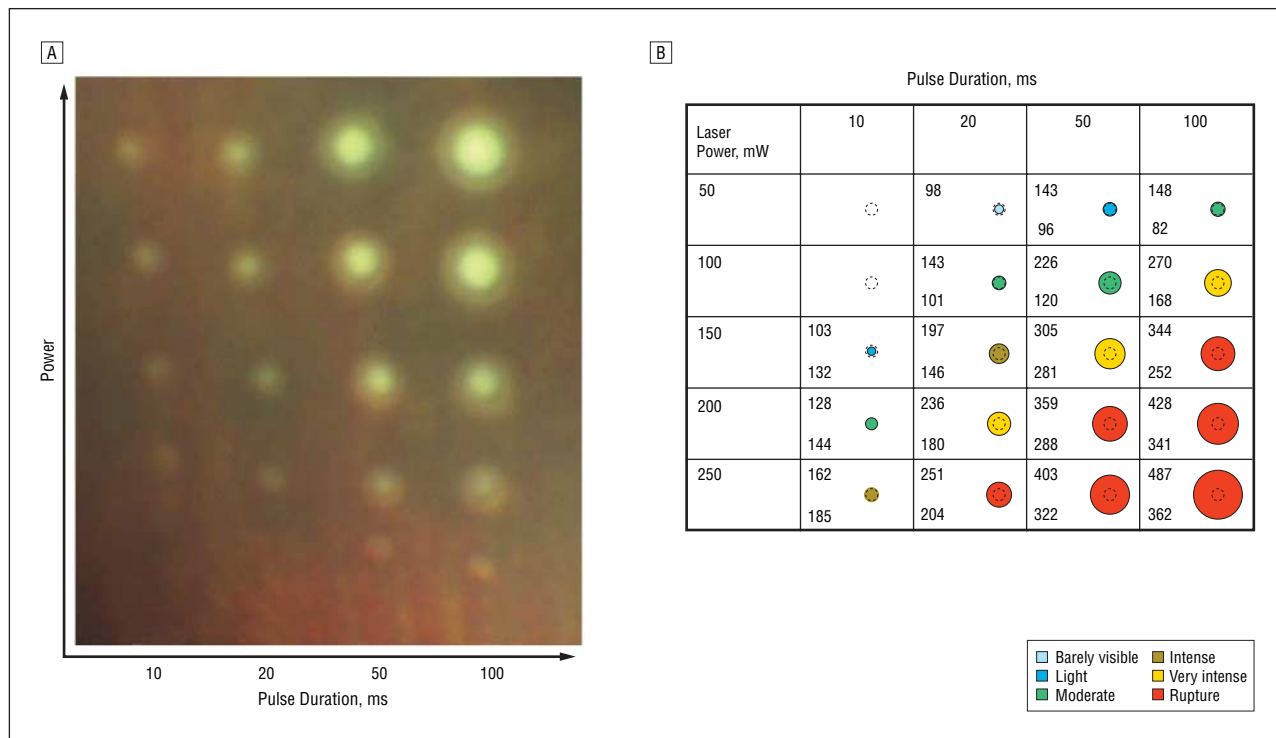


**Figure 1.** Photographic (A) and diagrammatic (B) representations of retinal photocoagulation lesion diameters (in micrometers) for a 132- $\mu\text{m}$  retinal beam size produced by different laser powers and durations. Dashed circles represent laser spot size at the retinal plane (132  $\mu\text{m}$ ); solid circles represent the final lesion size, as measured on fundus photographs (shown in the upper left corner of each box in B). The number in the lower left corner corresponds to histologic width of the damage zone. At 10-millisecond durations, histologic lesion sizes exceed the clinical appearance by about 15%. As pulse duration increased, the ratio of clinical width to histologic size increased, and at 100 milliseconds the clinical size of the lesion exceeded the histologic size by about 30%. The colors correspond to ophthalmoscopically graded lesion intensities (key). In most instances the rupture was much smaller than the width of the final lesion. No visible lesions could be obtained with 10-millisecond pulses at powers of 50 to 100 mW.

sion was one that just crossed the limit of clinical detection and produced no retinal whitening, whereas a mild lesion was described as one that produced some blanching but no whitening. A moderate lesion was one that produced some retinal whitening but did not have a ring of edema, while an intense lesion had an area of central whitening and a halo of translucent edema. A very intense lesion had a very pronounced area of opaque central retinal whitening and a larger ring of edema. A rupture was assumed when a vapor bubble or discontinuity in retinal architecture was visualized with or without bleeding.

Sets of lesions were imaged with the use of a digital camera attached to the slitlamp microscope at  $\times 10$  and  $\times 16$  magnification settings. At the lowest magnification setting, the diameter of even the smallest lesions spanned at least 20 pixels. The digital images were examined by means of the ImageJ software package (National Institutes of Health, Bethesda, Maryland).<sup>23</sup> The lesion size was defined as the geometric mean of the vertical and horizontal diameters, measured in pixels, at the full width of the background-corrected intensity profiles. Spatial calibration was achieved by similarly analyzing the image of a needle of known diameter placed on the retina, yielding a conversion factor of approximately 5  $\mu\text{m}/\text{pixel}$  at the  $10\times$  magnification setting. This corresponds to measurement precision of approximately  $\pm 5 \mu\text{m}$ .

## RESULTS

### RETINAL LESION SIZE

**Figure 1** provides photographic (A) and diagrammatic (B) representations, drawn to scale, of the retinal coagu-

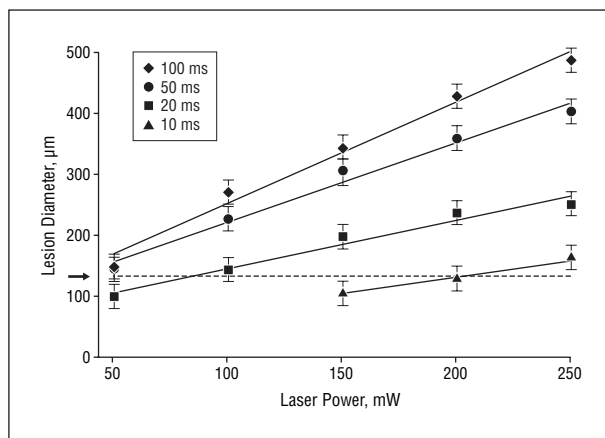


**Figure 2.** Clinical size of the retinal lesion plotted as a function of laser power for pulse durations ranging from 10 to 100 milliseconds with a retinal laser spot size of 132  $\mu\text{m}$ . The data can be approximated with linear functions; the slope increases with pulse duration. The dashed line represents a laser spot size of 132  $\mu\text{m}$  at the retinal plane.

lation lesions annotated in color to also indicate the clinical intensity (grade). Lesion size and clinical grade increased with both pulse duration and power.

At fixed pulse durations, the increase of the lesion size with laser power could be approximated by a linear function, as shown in **Figure 2** for a 132- $\mu\text{m}$  retinal laser spot size. Increases in size were more pronounced for longer pulse durations: the slopes of these linear fits in-

creased with pulse duration from 1.8  $\mu\text{m}/\text{mW}$  for 10-millisecond pulses to 3.3  $\mu\text{m}/\text{mW}$  for 100-millisecond pulses. Similar linear trends were observed for 66- $\mu\text{m}$  and 330- $\mu\text{m}$  retinal spot sizes as well (data not shown). As an example, for a 100-millisecond-duration pulse, the retinal lesion size increased from 148 to 487  $\mu\text{m}$  as the power increased from 50 to 250 mW, a change of almost 3.7-fold. In contrast, for a 10-millisecond pulse, the lesion size increased only from 103 to 162  $\mu\text{m}$ , or only 1.6-fold (Figure 2). While lesion sizes were roughly comparable at the lowest power settings for all pulse durations (98–148  $\mu\text{m}$  for a 132- $\mu\text{m}$  spot size), the clinical grades of these lesions were very different: the 10-millisecond exposure produced a barely visible lesion of 98  $\mu\text{m}$  and the 100-millisecond pulse resulted in a moderate lesion of 148  $\mu\text{m}$  (Figure 1).

The increase of lesion size associated with increasing pulse duration at constant power was best approximated by a logarithmic function (Figure 3). Data points for 10-millisecond laser exposures at 50 and 100 mW are not shown because clinically visible lesions could not be produced at these settings. Similar curves were observed for the other 2 spot sizes as well (data not shown).

#### HISTOLOGIC CHARACTERISTICS OF LASER LESIONS

Figure 4A is a histologic composite of retinal lesions produced by a 132- $\mu\text{m}$  beam at varying pulse durations and powers, as observed 1 hour after laser treatment. This sequence of images demonstrates the spread of the thermal injury both laterally and axially with increasing power for constant pulse duration in the columns. Maximal lateral extent of damage to the RPE–outer segment interface is indicated by a horizontal bar under each photograph. With pulses of shorter duration (10–20 milliseconds), the extent of this spread, similar to the clinical appearance represented in Figure 1, is less than with conventional 100-millisecond exposures. Viewed alternatively in rows rather than columns, the thermal damage zone also expanded with increasing pulse duration for each power level. At pulse durations of 50 to 100 milliseconds, thermal damage spreads from the RPE into the inner retina, including the nerve fiber layer. In contrast, at pulse durations of 10 milliseconds, the damage was principally limited to the outer retina. Similar spatial confinement with shorter exposures is also seen in the decreased axial extent of damage outwardly to the choroid. Higher magnification of 2 sections corresponding to the moderate to intense lesions produced by 10- and 100-millisecond exposures is shown in Figure 4B. As indicated by the arrows, 100-millisecond exposures affected all retinal layers, including both the nerve fiber layer and choroid. In contrast, the damage produced by 10-millisecond exposures was principally limited to the RPE and photoreceptor-associated layers. Arrows at the RPE layer indicate maximal lateral spread of damage to the outer segments. Arrows in the outer nuclear layer outline the zone of pyknotic nuclei of photoreceptors. Arrows above the retina show the lateral extent of changes in the ganglion cell layer and nerve fiber layer.

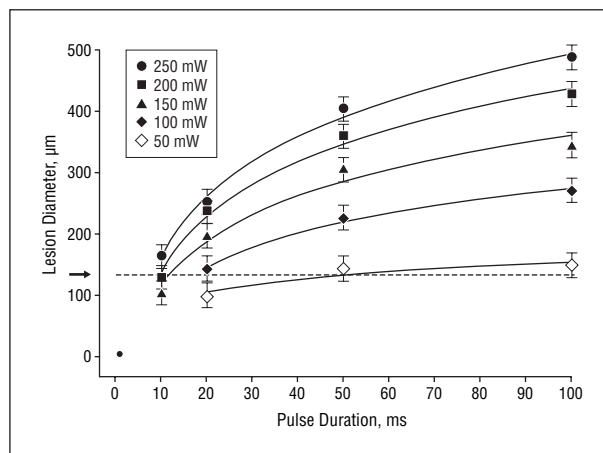


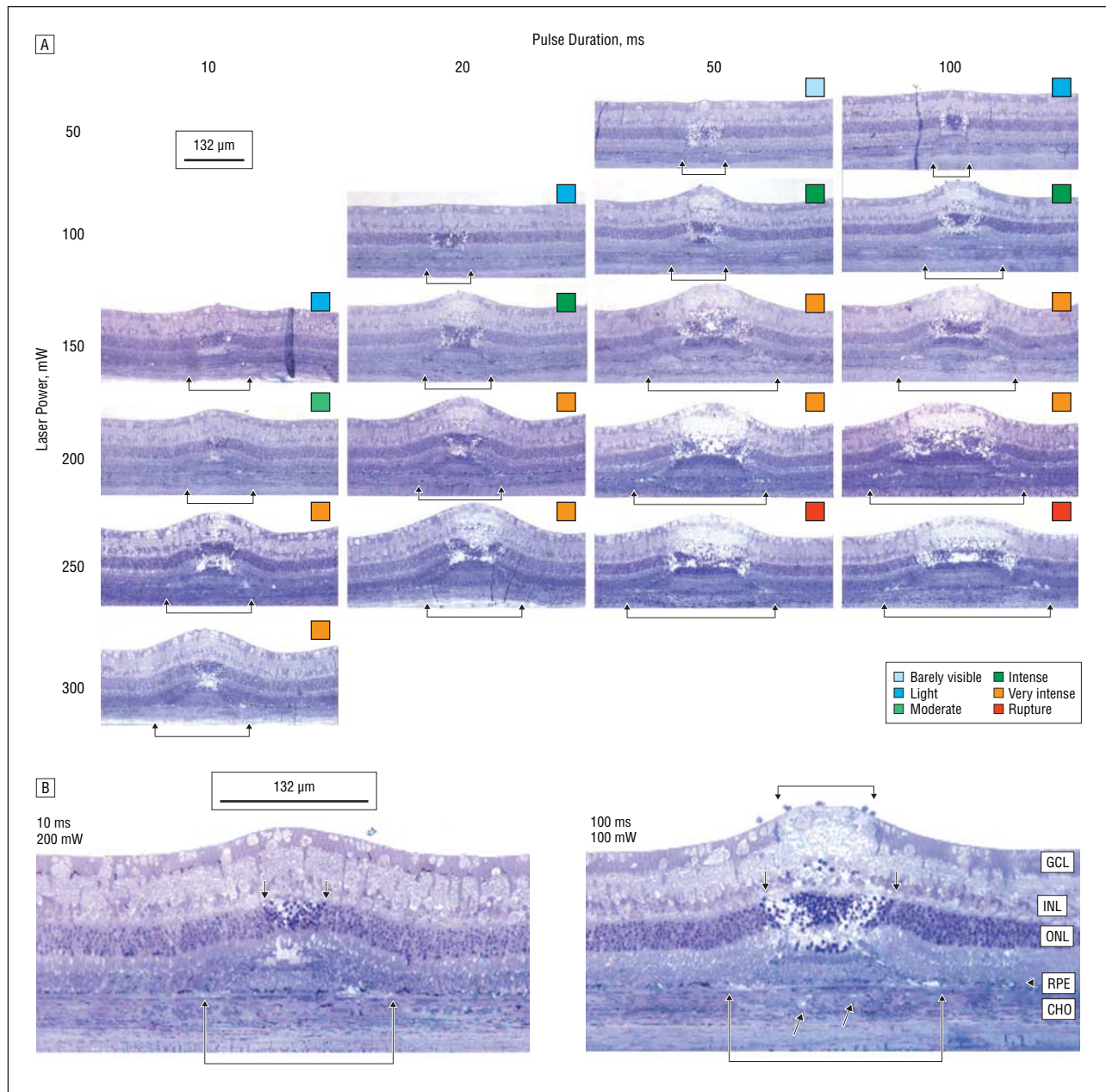
Figure 3. Clinical size of the retinal lesion plotted as a function of laser pulse duration for different laser power settings. The dashed line represents a laser spot size of 132  $\mu\text{m}$  at the retinal plane. Data were best fit by logarithmic functions.

Figure 5 demonstrates the typical histologic appearance encountered in mild retinal lesions 1 week after the treatment by laser pulses of various durations. All 4 lesions are significantly smaller than the laser beam size, shown as a white rectangle at the bottom of the upper section. Some retinal remodeling has begun, with resolution of the acute liquefactive changes and necrosis seen at 1 hour in most instances. Loss of photoreceptors has occurred in all lesions. Although all 4 sections exhibit some edema in the inner retina, with 10-millisecond pulses the bulk of the thermal damage is confined to primarily the RPE and photoreceptor layers, with the inner nuclear layer remaining largely intact. At 20-millisecond pulse durations, edema is seen in some sections in the inner nuclear layer, and with longer pulses the damage spreads more diffusely across the entire retina. At pulse durations of 100 milliseconds, extensive swelling and cystic changes in the ganglion cell layer can also be seen. Arrows in the 50- and 100-millisecond sections point to affected areas in the inner nuclear layer and ganglion cell layer.

#### RETINAL COAGULATION THRESHOLDS AND THE THERAPEUTIC WINDOW

Figure 6A depicts the power thresholds for creation of each of the grades of the retinal lesions as a function of pulse duration for a 132- $\mu\text{m}$  retinal laser spot size. A relatively modest power increase is required to produce comparable lesion grades going from 100 milliseconds to 10 milliseconds, whereas a much steeper increase is seen for durations under 10 milliseconds. The threshold pulse energy increases with pulse duration (Figure 6B), which is expected because of the increasing role of heat diffusion with longer pulses. For pulse durations of 20, 50, and 100 milliseconds, all the grades (mild, moderate, intense, very intense, and rupture) could be created with the appropriate choice of power settings. At pulse durations less than 10 milliseconds, it became increasingly difficult to reproducibly create intense or very intense lesions without inadvertently rupturing the retina. At 2 mil-





**Figure 4.** Histologic sections of rabbit retinas 1 hour after treatment with a 132- $\mu$ m retinal spot size. A, Composite histologic appearance for different pulse durations and powers. Each column corresponds to constant pulse duration, and each row to a constant power. Horizontal bars under each section demarcate the maximal lateral extent of damage at the retinal pigment epithelium (RPE)/outer segment interface. The colored square in the upper right corner of each image corresponds to the ophthalmoscopic grade of the lesion (key). Scale bar of 132  $\mu$ m corresponds to the beam size. B, Magnified view of 2 moderate to intense lesions. The 100-millisecond exposure produced damage not only to RPE and photoreceptors, but also to choroid (CHO) and inner retina (arrows). Damage produced by the 10-millisecond exposure is limited to RPE and photoreceptors. GCL indicates ganglion cell layer; INL, inner nuclear layer; and ONL, outer nuclear layer.

liseconds or less, it was not possible to reproducibly create an intense lesion without rupturing the retina. An even more abrupt decrease in the dynamic range of achievable lesions occurred at 1 millisecond, where there was little or no difference between the power required to create a mild retinal lesion and that to produce a rupture.

We refer to the ratio of the threshold power required to produce a rupture to that required to produce a mild lesion as the *therapeutic window*, and it represents one means of quantifying the relative safety (dynamic range) of retinal photocoagulation. The larger this ratio or therapeutic window, the greater the margin of safety to cre-

ate a visible lesion without inadvertently inducing a retinal rupture. **Figure 7** depicts the width of this window (and, by extension, safety) as a function of pulse duration for 2 different laser spot sizes. For a 132- $\mu$ m retinal laser beam size, as pulse duration decreases from 100 to 20 milliseconds, the width of the therapeutic window declines from 3.9 to 3.0. When pulse duration is further decreased to 10 milliseconds, the therapeutic window decreases to 2.5, and it approaches unity at pulse durations of 1 millisecond. At this point, there is effectively no safe range of retinal photocoagulation: mild lesion and rupture are equally likely to occur at the same power.

The width of the therapeutic window for a 330- $\mu\text{m}$  retinal laser spot size is greater than that of a 132- $\mu\text{m}$  retinal spot. It declines from 5.4 to 3.7 to 3.1 when pulse durations decrease from 100 to 20 to 10 milliseconds, respectively. Similar to the smaller spot sizes, the therapeutic window for visible lesions decreases to unity as pulse durations decrease to 1 millisecond.

### COMMENT

The results of our study demonstrate that not only the laser beam size but also pulse duration and power strongly affect the final size of the retinal lesion. The increase of the lesion size with laser power for each pulse duration ranging between 10 and 100 milliseconds could be approximated by a linear function, with the rate of this increase being greater for longer pulses. As a result, final lesion sizes for 50- to 100-millisecond pulses exceed the retinal beam size by a factor of 3 or more. In contrast, at shorter pulses (10-20 milliseconds), the lesion sizes vary much less with laser power and remain comparable to the spot diameter (Figure 3). Because the amount of heat generated in the pigmented layers increases with absorption coefficient and laser power, variations in pigmentation will affect lesion characteristics, as do variations of laser power. Thus, retinal lesions in the areas with variable pigmentation are expected to have more uniform sizes at shorter pulse durations than conventional longer durations.

Although ophthalmoscopic and histologic sizes correlated well, they were not identical. At longer pulse durations, the ophthalmoscopic size of the retinal lesion exceeded the histologic estimates (on the order of 25%). This ratio decreased with shorter pulses, and at 10 milliseconds the ophthalmoscopic appearance of the lesion was actually smaller than the histologic measurement by approximately 15%. This trend would be expected to continue with decreasing pulse durations, whereby retinal damage would be increasingly confined to RPE because of the reduced effects of heat diffusion. Such confinement contributes to the lesions being less visible ophthalmoscopically. Thermal diffusion length  $L$  scales as square root of the pulse duration  $t$ :

$$L = \sqrt{4kt},$$

where  $k$  is thermal diffusivity of tissue.<sup>24</sup> Because the retina has about 90% water content, its thermal diffusivity is close to that of water ( $k=0.14 \text{ mm}^2/\text{s}$ ). Heat generated by melanin absorption in the RPE will not diffuse beyond a single cellular layer ( $L=7 \mu\text{m}$ ) during the laser pulse if its duration does not exceed 0.1 millisecond. With pulses of 10 milliseconds, the diffusion length would be expected to be approximately 70  $\mu\text{m}$ . Decrease of the lateral temperature gradient with increasing pulse duration may account for the smoother edges of the coagulation lesions with longer pulse durations as compared with shorter ones.

The rate of retinal coagulation can be estimated by means of the Arrhenius equation,<sup>24,25</sup> with a total integral of damage:

$$\Omega_{\text{threshold}} = A \int_0^{\tau} \exp\left(-\frac{E^*}{kT(t)}\right) dt,$$

where  $A$  is a rate constant;  $E^*$ , excitation energy;  $k$ , Boltzmann constant;  $T$ , temperature; and  $\tau$ , total duration of

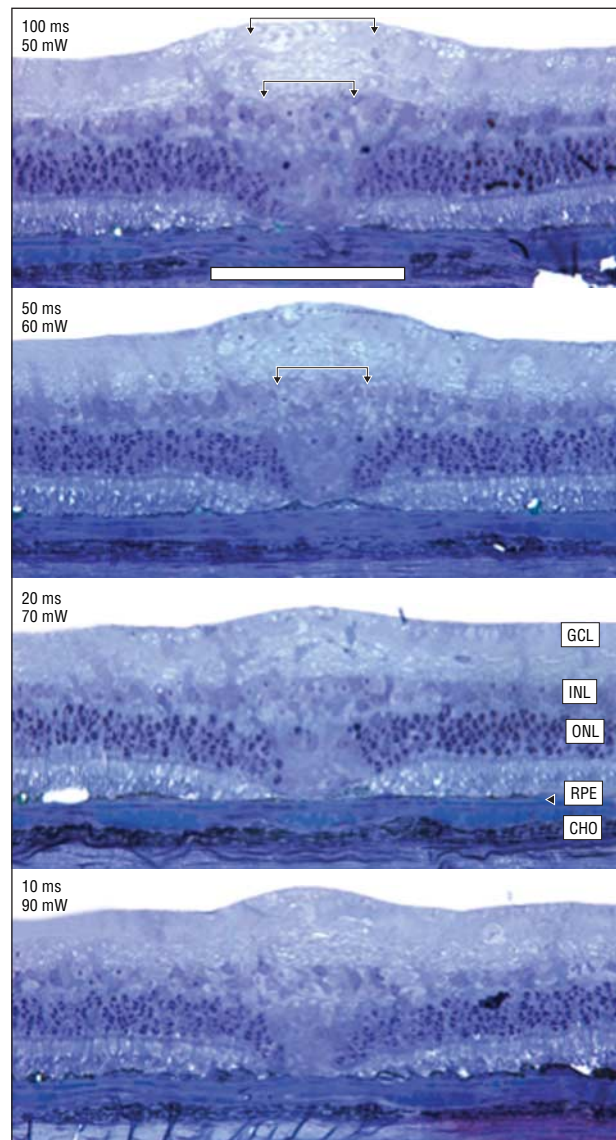


**Figure 5.** Histologic appearance of retinal lesions graded as mild (light) to moderate 1 week after irradiation with differing combinations of pulse duration and power required to obtain an approximately equal ophthalmoscopic end point. Corresponding pulse duration and power are shown in the left upper corner of each section. Some retinal remodeling has begun, with resolution of the acute liquefactive changes and necrosis seen at 1 hour in most instances. Loss of photoreceptors has occurred in all lesions. However, preservation of the inner and middle retinal layers and nuclei appears to be greater with lower pulse duration and higher power than with longer pulse duration and lower power. See Figure 4 for abbreviations.

hyperthermia, which includes heating and cooling phases. As laser pulse duration and associated duration of hyperthermia decrease, the temperature required for achieving the same value of the damage integral  $Q$  has to increase, so higher laser power will be required. However, as soon as the temperature exceeds the vaporization threshold, vapor bubbles will produce retinal rupture. Thus, the safe range of retinal coagulation, namely, the range of power sufficient for coagulation but not exceeding the threshold of retinal rupture, is expected to decrease with decreasing pulse durations.<sup>7</sup>

The clinical implications of these findings are potentially important. From a practical standpoint, when shorter

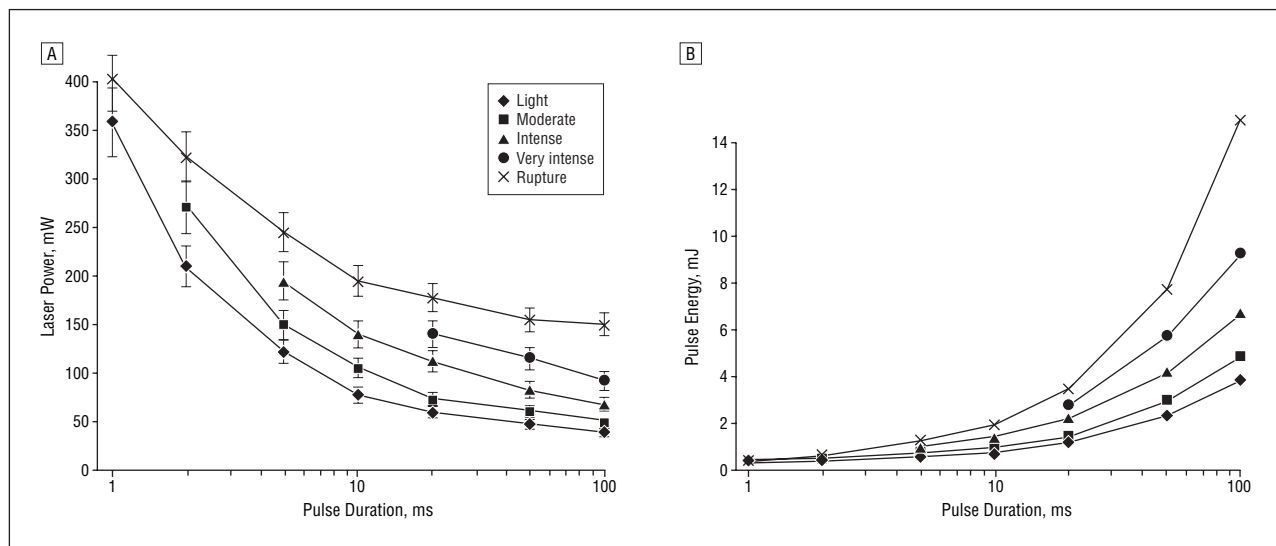


**Figure 6.** Semilogarithmic plots of retinal coagulation thresholds. A, Power thresholds for various grades of retinal lesions as a function of pulse duration. Higher powers are required to produce a rupture compared with mild or moderate lesions for comparable pulse durations. As pulse duration decreases, these differences decrease. Data were obtained with a retinal spot size of 132  $\mu\text{m}$  and are presented as mean thresholds with standard deviations. B, Threshold pulse energies for various grades of retinal lesions as a function of pulse duration. Pulse energy required for producing equivalent grades of lesions increases with pulse duration, indicating an increasing role of heat diffusion with longer exposures.

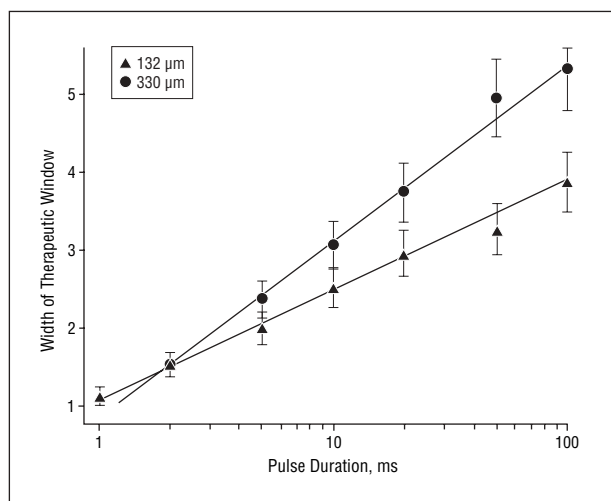


**Figure 7.** Semilogarithmic plot of the width of the therapeutic window (the ratio of the threshold of rupture to that of a mild [light] coagulation lesion) as a function of pulse duration for retinal laser spot sizes of 132 and 330  $\mu\text{m}$ .

exposures (10-20 milliseconds) are used with a conventional single-spot delivery or a pattern scanning system, the retinal lesion size will be smaller than the clinician typically encounters with conventional durations of 100 to 200 milliseconds. Therefore, more lesions or a larger spot size may be required to achieve equal retinal treatment area. Another factor favoring the choice of larger beam size is the greater width of the therapeutic window (Figure 7).

As noted in Figure 1 and Figure 6, with a retinal beam size of 132  $\mu\text{m}$  and pulses of 20 milliseconds, all grades of lesions could be produced, while, with shorter pulses, fewer and fewer grades could be achieved below the threshold of rupture. The width of the therapeutic window, for that spot size, defined as the ratio of the threshold of rupture to that of a mild lesion, exceeds 3 at all

pulse durations greater than 20 milliseconds. With a beam size of 330  $\mu\text{m}$ , similar performance could be achieved with all pulses longer than 10 milliseconds. These data suggest that 10 to 20 milliseconds represents an optimal range of duration as a compromise between treatment speed and spatial confinement of the lesion on one hand and sufficient safety range for avoiding inadvertent ruptures on the other. It would not be possible to efficiently scan patterns of more than a few spots without danger of inadvertent eye movement and resulting spot misplacement with the use of much longer pulse durations.

Pulses in the range of 10 to 20 milliseconds, even when delivered as single spots rather than a pattern, may prove advantageous relative to conventional durations. This is because of not only better predictability of the lesion size and its ophthalmoscopic uniformity but also decreased axial spread of heat toward the choroid and toward the inner retinal layers (Figure 4B and Figure 5). Better spatial confinement of the lesion may translate into less damage to the nerve fiber layer and decreased choroidal swelling, although this will need to be confirmed in a clinical trial. Reduced pain, presumably associated with less choroidal heating and nerve injury, has been noted in humans undergoing photocoagulation with pulse durations of 10 to 20 milliseconds.<sup>5,17</sup>

The retinal coagulation lesions applied in this study were confined to the area of the visual streak adjacent to the medullary ray in rabbits. Important limitations exist with regard to the extrapolation of this data from rabbits to humans. It has been observed clinically in humans that the lesion grades are enhanced in more peripheral areas of the fundus compared with the posterior retina.

In summary, our data suggest that pulse durations of about 20 milliseconds provide several advantages over the conventional 100-millisecond duration with regard to the predictability of the lesion size, reduction in col-



lateral injury through reduced axial and lateral spread of heat, and ability to pattern scan during the eye fixation time. Reduced penetration of heat into the choroid has the potential to decrease pain, although further clinical studies will be required to substantiate these predicted benefits. It should also be emphasized that larger laser spot sizes are needed to coagulate the same amount of tissue when shorter pulses are applied.

**Submitted for Publication:** October 28, 2006; final revision received June 26, 2007; accepted July 4, 2007.

**Correspondence:** Daniel Palanker, PhD, Department of Ophthalmology, Stanford University, 300 Pasteur Dr, Room A157, Stanford, CA 94305-5308 (palanker@stanford.edu).

**Financial Disclosure:** Drs Blumenkranz and Palanker are parties to a Stanford University patent on patterned scanning laser photocoagulation licensed to OptiMedica Corp with an associated equity and royalty interest, and serve as consultants for OptiMedica Corp. Messrs Wiltberger and Andersen are employees of OptiMedica Corp.

**Funding/Support:** This study was supported by an Alcon Research Institute grant and by charitable gifts of the Horngren and Miller Family Foundations.

**Additional Contributions:** Michael Marmor, MD, and Boris Stanzel, MD, helped with analysis of retinal pathology. Roopa Dalal, MSc, assisted with histologic preparations.

## REFERENCES

- Little HL, Zweng HC, Peabody RR. Argon laser slit-lamp retinal photocoagulation. *Trans Am Acad Ophthalmol Otolaryngol.* 1970;74(1):85-97.
- Early Treatment Diabetic Retinopathy Study Research Group. Treatment techniques and clinical guidelines for photocoagulation of diabetic macular edema: Early Treatment Diabetic Retinopathy Study Report Number 2. *Ophthalmology.* 1987;94(7):761-774.
- Macular Photocoagulation Study Group. The influence of treatment extent on the visual acuity of eyes treated with krypton laser for juxtafoveal choroidal neovascularization. *Arch Ophthalmol.* 1995;113(2):190-194.
- Kapany NS, Peppers NA, Zweng HC, Flocks M. Retinal photocoagulation by lasers. *Nature.* 1963;199:146-149.
- Mainster MA. Decreasing retinal photocoagulation damage: principles and techniques. *Semin Ophthalmol.* 1999;14(4):200-209.
- Obana A, Lorenz B, Gassler A, Birngruber R. The therapeutic range of chorioretinal photocoagulation with diode and argon lasers: an experimental comparison. *Lasers Light Ophthalmol.* 1992;4(3/4):147-156.
- Birngruber R, Gabel VP, Hillenkamp F. Fundus reflectometry: a step towards optimization of the retina photocoagulation. *Mod Probl Ophthalmol.* 1977;18:383-390.
- Smiddy WE, Fine SL, Quigley HA, Hohman RM, Addicks EA. Comparison of krypton and argon laser photocoagulation: results of stimulated clinical treatment of primate retina. *Arch Ophthalmol.* 1984;102(7):1086-1092.
- Smiddy WE, Patz A, Quigley HA, Dunkelberger GR. Histopathology of the effects of tuneable dye laser on monkey retina. *Ophthalmology.* 1988;95(7):956-963.
- Palanker D, Blumenkranz MS, Weiter JJ. Retinal laser therapy: biophysical basis and applications. In: Ryan SJ, Schachat AP, Wilkinson WP, Glaser B, eds. *Retina.* 4th ed. St Louis, MO: Elsevier Health Sciences; 2005: 539-553.
- Roeder J, Hillenkamp F, Flotte T, Birngruber R. Microphotocoagulation: selective effects of repetitive short laser pulses. *Proc Natl Acad Sci U S A.* 1993;90(18):8643-8647.
- Luttrull JK, Musch DC, Mainster MA. Subthreshold diode micropulse photocoagulation for the treatment of clinically significant diabetic macular oedema. *Br J Ophthalmol.* 2005;89(1):74-80.
- Desmettre TJ, Mordon SR, Buzawa DM, Mainster MA. Micropulse and continuous wave diode retinal photocoagulation: visible and subvisible lesion parameters. *Br J Ophthalmol.* 2006;90(6):709-712.
- Framme C, Schuele G, Roeder J, Birngruber R, Brinkmann R. Influence of pulse duration and pulse number in selective RPE laser treatment. *Lasers Surg Med.* 2004;34(3):206-215.
- Framme C, Schuele G, Roeder J, Kracht D, Birngruber R, Brinkmann R. Threshold determinations for selective retinal pigment epithelium damage with repetitive pulsed microsecond laser systems in rabbits. *Ophthalmic Surg Lasers.* 2002;33(5):400-409.
- Schuele G, Rumohr M, Huettmann G, Brinkmann R. RPE damage thresholds and mechanisms for laser exposure in the microsecond-to-millisecond time regimen. *Invest Ophthalmol Vis Sci.* 2005;46(2):714-719.
- Blumenkranz MS, Yellachich D, Andersen DE, et al. Semiautomated patterned scanning laser for retinal photocoagulation. *Retina.* 2006;26(3):370-376.
- Mosier MA, Champion J, Liaw LH, Berns MW. Retinal effects of the frequency-doubled (532 nm) YAG laser: histopathological comparison with argon laser. *Lasers Surg Med.* 1985;5(4):377-404.
- McMullen WW, Garcia CA. Comparison of retinal photocoagulation using pulsed frequency-doubled neodymium-YAG and argon green laser. *Retina.* 1992;12(3):265-269.
- Mainster MA. Wavelength selection in macular photocoagulation: tissue optics, thermal effects, and laser systems. *Ophthalmology.* 1986;93(7):952-958.
- Birngruber R. Choroidal circulation and heat convection at the fundus of the eye. In: Wolbarsht ML, ed. *Laser Applications to Medicine and Biology.* New York, NY: Plenum Press; 1991:277-361.
- Turner KW. Hematoxylin toluidine blue-phloxinate staining of glycol methacrylate sections of retina and other tissues. *Stain Technol.* 1980;55(4):229-233.
- National Institutes of Health. ImageJ. Published 2004. <http://rsb.info.nih.gov/ij/index.html>. Accessed October 25, 2007.
- Niemz M. Heat transport. In: Greenbaum E, ed. *Laser-Tissue Interactions: Fundamentals and Applications.* Berlin, Germany: Springer; 2002:68-80. Biological and Medical Physics Series.
- Birngruber R, Hillenkamp F, Gabel VP. Theoretical investigations of laser thermal retinal injury. *Health Phys.* 1985;48(6):781-796.